LBNL-40254
UC-414
Preprint

Ernest Orlando Lawrence Berkeley National Laboratory

Electron Injection into Plasma Wakefields by Colliding Laser Pulses

W.P. Leemans, E. Esarey, R.F. Hubbard, A. Ting, and P. Sprangle
Accelerator and Fusion Research Division

May 1997
Submitted to
Physical Review Letters

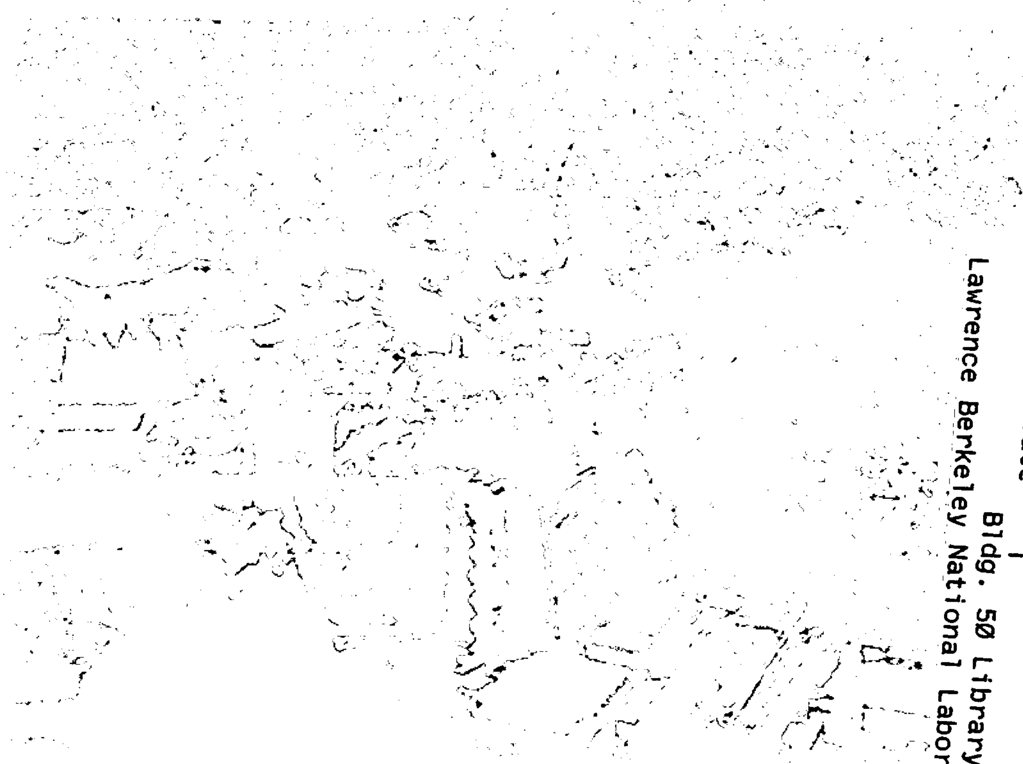

DISCLAIMER

LBNL-40254
CBP Note-223

Electron Injection into Plasma Wakefields by Colliding Laser Pulses*

W. P. Leemans
Lawrence Berkeley National Laboratory
University of California,
Berkeley, California 94720

E. Esarey, R. F. Hubbard, A. Ting, and P. Sprangle
Naval Research Laboratory
Washington D. C. 20375-5346

May 1997

submitted to *Physical Review Letters*

* This work was supported by the Director, Office of Energy Research, Office of High Energy and Nuclear Physics, High Energy Physics Division, of the U. S. Department of Energy, under Contract No. DE-AC03-76SF00098.

Electron Injection into Plasma Wakefields by Colliding Laser Pulses

E. Esarey, R.F. Hubbard, W.P. Leemans,* A. Ting, and P. Sprangle

Beam Physics Branch, Plasma Physics Division
Naval Research Laboratory, Washington DC 20375-5346

**Ernest Orlando Lawrence Berkeley National Laboratory*
University of California at Berkeley, Berkeley CA 94720

Abstract

An injector and accelerator is analyzed that uses three collinear laser pulses in a plasma: an intense pump pulse, which generates a large wakefield ($\geq$ 15 GV/m), and two counterpropagating injection pulses. When the injection pulses collide, a slow phase velocity ponderomotive wave is generated that injects electrons into the fast wakefield for acceleration. For injection pulse intensities of 5×10^{16} W/cm^2 and wakefield amplitudes of $\delta n/n \simeq 0.6$, the production of ultrashort ($\leq$ 20 fs) relativistic electron bunches with energy spreads $\leq 20\%$ and densities $\geq 10^{17}$ cm^{-3} appears possible.

Plasma-based accelerators [1] may provide a compact source of high energy electrons due to their ability to sustain ultrahigh accelerating fields E_z on the order of $E_0 = cm_e\omega_p/e \simeq n_0^{1/2}[\mathrm{cm}^{-3}]$ V/cm, where $\omega_p = (4\pi n_0 e^2/m_e)^{1/2}$ is the plasma frequency and n_0 is the plasma density. Accelerating fields of 10-100 GV/m have been generated over distances of a few mm [2-4] in both the standard [5] and self-modulated [6,7] regimes of the laser wakefield accelerator (LWFA). The characteristic scalelength of the accelerating plasma wave is the plasma wavelength $\lambda_p = 2\pi c/\omega_p$, which is typically $\lesssim 100$ μm. Although several recent experiments [3,4] have demonstrated the self-trapping and acceleration of plasma electrons in the self-modulated LWFA, the production of electron beams with relatively low momentum spread and good pulse-to-pulse energy stability will require injection of ultrashort electron bunches into the wakefield with femtosecond timing accuracy. These requirements are beyond the current state-of-the-art performance of photo-cathode radio-frequency electron guns.

Recently an all-optical method for injecting electrons in a standard LWFA has been proposed [8]. This method (referred to as LILAC) utilizes two laser pulses which propagate either perpendicular or parallel to one another. The first pulse (the pump pulse) generates the wakefield, and the second pulse (the injection pulse) intersects the wakefield some distance behind the pump pulse. The ponderomotive force $F_p \sim \nabla a^2$ of the injection pulse can accelerate a fraction of the plasma electrons such that they become trapped in the wakefield, where $a^2 \simeq 7 \times 10^{-19}\lambda^2[\mu\mathrm{m}]I[\mathrm{W/cm}^2]$, $\lambda = 2\pi c/\omega$ is the laser wavelength, and I the intensity. Simulations, which were performed for ultrashort pulses at high densities ($\lambda_p/\lambda = 10$ and $E_z/E_0 = 0.7$), indicated the production of a 10 fs, 21 MeV electron bunch with a 6% energy spread. However, high intensities ($I > 10^{18}$ W/cm^2) are required in both the pump and injection pulses ($a \simeq 2$). An all optical electron injector would be a significant step in reducing the size and cost of a LWFA.

In the following, a colliding pulse optical injection scheme for a LWFA is proposed and analyzed which makes use of a two-stage acceleration process. Three short laser pulses are employed: an intense pump pulse (denoted by subscript 0), a forward going injection pulse (subscript 1), and a backward going injection pulse (subscript 2), as shown in Fig. 1. The frequency, wavenumber, and normalized intensity are denoted by ω_i, k_i, and a_i ($i = 0, 1, 2$). Furthermore, $\omega_1 = \omega_0$, $\omega_2 = \omega_0 - \Delta\omega$ ($\Delta\omega \geq 0$), and $\omega_0 \gg \Delta\omega \gg \omega_p$ will be assumed such that $k_1 = k_0$, and $k_2 \simeq -k_0$. The pump pulse generates a fast ($v_{p0} \simeq c$) wakefield. When the injection pulses collide (some distance behind the pump) they generate a slow ponderomotive beat wave with a phase velocity $v_{pb} \simeq \Delta\omega/2k_0$. During the time in which the two injection pulses overlap, a two-stage acceleration process can occur, i.e., the slow beat wave can inject plasma electrons into the fast wakefield for acceleration to high energies. It will be shown that injection and acceleration can occur at low densities ($\lambda_p/\lambda \sim 100$), thus allowing for high single-stage energy gains, with normalized injection pulse intensities of $a_1 \sim a_2 \sim 0.2$, i.e., two orders of magnitude less intensity than required by the LILAC scheme.

A somewhat analogous two-stage acceleration process can lead to self-trapping in the self-modulated LWFA due to the interaction of the Raman backscatter (RBS) waves with the wakefield [4,9,10]. In the self-modulated LWFA [6,7], the plasma density n_0 is sufficiently high ($\lambda_p/\lambda \sim 10$) such that $L > \lambda_p$, where L is the laser pulse length. Since

$L > \lambda_p$, RBS readily occurs, which involves the decay of the pump laser light (ω, k) into backward light $(\omega - \omega_p, -k)$ and a plasma wave $(\omega_p, 2k)$ [1]. The slow $(v_p = \omega_p/2k)$ RBS plasma wave can preheat the plasma such that a fraction of the electrons are accelerated to high energies in the fast $(v_p \simeq c)$ wakefield [4,9,10]. Dephasing limits the electron energy gain to $W_d \simeq 4m_ec^2\lambda_p^2 E_z/\lambda^2 E_0 \sim n_0^{-1}$, which is relatively low ($W_d \sim 100$ MeV) at high densities [1]. Higher single-stage energy gains can be obtained at lower plasma densities as in the standard LWFA [5], in which $L \simeq \lambda_p$ $(\lambda_p/\lambda \sim 100)$. Since $L \simeq \lambda_p$, Raman instabilities will be suppressed and self-trapping of plasma electrons is unlikely. Acceleration in the standard LWFA requires an additional injection mechanism.

The colliding pulse injection mechanism will be analyzed in one-dimension (1-D) with the plasma wave and laser fields represented by the normalized scalar $\phi = e\Phi/m_ec^2$ and vector $\mathbf{a} = e\mathbf{A}_\perp/m_ec^2$ potentials, respectively. The axial component of the normalized electron momentum $u_z = p_z/m_ec = \gamma\beta_z$ obeys

$$\frac{du_z}{dct} = \frac{\partial \phi}{\partial z} - \frac{1}{2\gamma}\frac{\partial a^2}{\partial z}, \tag{1}$$

where $\gamma = \gamma_z\gamma_\perp$, $\gamma_\perp = (1+a^2)^{1/2}$, and $\gamma_z = (1-\beta_z^2)^{-1/2}$. In terms of the phase of the electron with respect to the wakefield $\psi = k_p(z - v_{p0}t)$, Eq. (1) can be written as

$$\frac{d^2\psi}{d\tau^2} = \frac{(1-\beta_z^2)}{\gamma}\frac{\partial \phi}{\partial \hat{z}} - \frac{1}{\gamma^2}\left(\frac{\partial}{\partial \hat{z}} + \beta_z\frac{\partial}{\partial \tau}\right)\frac{a^2}{2}, \tag{2}$$

where $k_p = \omega_p/c$, $v_{p0} = c\beta_{p0}$ is the wakefield phase velocity, $\hat{z} = k_pz$, $\tau = \omega_pt$, and $\beta_z = d\psi/d\tau + \beta_{p0}$.

The effects of three waves will be considered: a plasma wakefield $\phi = \hat{\phi}(\psi)\cos\psi$, and a forward and a backward injection laser pulse, both of the form $\mathbf{a}_i = \hat{a}_i(z -$

$v_{gi}t)(\sin\theta_i \mathbf{e}_x + \cos\theta_i \mathbf{e}_y)$. Here, $\theta_i = k_i z - \omega_i t$ and the amplitudes $\hat{a}_i$ and $\hat{\phi}$ are assumed to be slowly varying compared to the phases θ_i and ψ. Also, k_i and ω_i satisfy $k_i = \sigma_i \omega_i (1 - \omega_p^2/\omega_i^2)^{1/2}$, where $\sigma_1 = 1$ and $\sigma_2 = -1$, which implies a group velocity $v_{gi} = c\beta_{gi} = c^2 k_i/\omega_i$ ($v_{p0} = v_{g0} = v_{g1}$). Furthermore, $a^2 = \hat{a}_1^2 + \hat{a}_2^2 + 2\hat{a}_1\hat{a}_2\cos\psi_b$, where $\psi_b = \theta_1 - \theta_2 = \Delta k(z - v_{pb}t)$ is the beat phase, $v_{pb} = c\beta_{pb} = \Delta\omega/\Delta k$, and $\Delta k = k_1 - k_2 \simeq 2k_0$. To leading order, Eq. (2) becomes

$$d^2\psi/d\tau^2 \simeq b_0\hat{\phi}\sin\psi + b_1(\Delta k/k_p)\hat{a}_1\hat{a}_2\sin\psi_b, \tag{3}$$

where $b_0 = -\gamma_\perp^{-1}(1-\beta_z)^{3/2}$, $b_1 = \gamma_\perp^{-2}(1-\beta_z^2)(1-\beta_{pb}\beta_z)$, and $\psi_b = [(\beta_{p0}-\beta_{pb})\tau + \psi]\Delta k/k_p$.

The ponderomotive force of the injection laser pulses can also lead to the generation of space charge fields via $(\partial^2/\partial t^2 + \omega_p^2)\phi_s = \omega_p^2 a^2/2$. The beat wave term $2\hat{a}_1\hat{a}_2\cos\psi_b$ will generate a space charge wave with an amplitude $|\phi_s| < (\omega_p/\Delta\omega)^2\hat{a}_1\hat{a}_2$. The force arising from ϕ_s is smaller than that of the beat wave by at least $(\omega_p/\Delta\omega)^2 \ll 1$ and will be neglected in the following.

In the absence of the injection pulses, electron motion in the wakefield is described by the Hamiltonian [11] $H_w = \gamma - \beta_{p0}(\gamma^2 - 1)^{1/2} - \phi$, where $\phi = \phi_0\cos\psi$. In (γ, ψ) phase space, unstable fixed points (x-points) occur at $\gamma = \gamma_{p0}$ and $\psi = \pi \pm 2\pi j$ and stable fixed points (o-points) occur at $\gamma = \gamma_{p0}$ and $\psi = \pm 2\pi j$ ($j = 0, 1, 2...$), where $\gamma_{p0} = (1 - \beta_{p0}^2)^{-1/2}$. The boundary between trapped and untrapped orbits is given by the separatrix $H_w(\gamma, \psi) = H_w(\gamma_{p0}, \pi)$. The minimum momentum of an electron on the separatrix is given by $u_{min} \simeq (1/\Delta\phi - \Delta\phi)/2$, where $\Delta\phi = \phi_0(1 + \cos\psi)$, assuming $\gamma_{p0}\Delta\phi \gg 1$ and $\beta_{p0} \simeq 1$. In particular at $\psi = 0$, $u_{min} = 0$ for $\phi_0 = 1/2$, which means that an electron that is at rest at the phase $\psi = 0$ will be trapped. The background plasma electron, however, are untrapped and are undergoing a fluid oscillation with a momentum $u_f \simeq -\phi$ ($\phi^2 \ll 1$). Hence, at $\psi = 0$, the plasma electrons are moving backward with $u_f \simeq -\phi_0$, which is far from the trapping threshold (see Fig. 2).

The beat wave leads to formation of phase space buckets (separatrices) of width $2\pi/\Delta k \simeq \lambda_0/2$, which are much shorter than those of the wakefield (λ_p), thus allowing for a separation of time scales. In particular, it can be shown that both the transit time $2\pi/\Delta\omega$ of an untrapped electron through a beat wave bucket and the synchrotron (bounce) time $\pi/(\hat{a}_1\hat{a}_2)^{1/2}\omega_0$ of a deeply trapped electron in a beat wave bucket are much shorter than a plasma wave period $2\pi/\omega_p$. Hence, on the time scale in which an electron interacts with a single beat wave bucket, the wakefield electric field can be approximated as static.

In the combined fields, the electron motion can be analyzed in the local vicinity of a single period of the beat wave by assuming that the wakefield electric field $E_z = -k_p^{-1}E_0\partial\phi/\partial z \simeq E_{z0}$ is constant. The Hamiltonian associated with Eq. (3) is given by

$$H_b = \gamma - \beta_{pb}\left[\gamma^2 - \gamma_\perp^2(\psi_b)\right]^{1/2} + \epsilon\psi_b, \tag{4}$$

where $\epsilon = E_{z0}k_p/E_0\Delta k$ is constant and $\gamma_\perp^2 = 1 + \hat{a}_1^2 + \hat{a}_2^2 + 2\hat{a}_1\hat{a}_2\cos\psi_b$. When $\epsilon = 0$, the phase space orbits are symmetric with x-points at $\beta_z = \beta_{pb}$, $\psi_b = \pm 2\pi j$ and o-points at $\beta_z = \beta_{pb}$, $\psi_b = \pi \pm 2\pi j$. When $\epsilon \neq 0$, the separatrix distorts into fished-shape islands (see Fig. 2). When $\epsilon < 0$ ($\epsilon > 0$), the "fish tail" of the separatrix opens to the right (left). In terms of the normalized axial momentum, the maximum and minimum points on the separatrix, u_{bm}, obtained from Eq. (4), are given by

$$u_{bm} \simeq \beta_{pb}(\gamma_0 - \pi\gamma_{pb}^2|\epsilon|) \pm 2\hat{a}_1^2\gamma_{pb}\left(1 - \pi\gamma_0|\epsilon|/2\hat{a}_1^2\right)^{1/2}, \tag{5}$$

where $\gamma_0 = \gamma_{bp}(1+4\hat{a}_1^2)^{1/2}$, $\gamma_{pb} = (1-\beta_{pb}^2)^{-1/2}$, $\pi\gamma_0|\epsilon|/2\hat{a}_1^2 < 1$, and $\hat{a}_1 = \hat{a}_2$ are assumed.

A scenario by which the beat wave leads to trapping in the plasma wave is the following. In the phase region $-\pi/2 < \psi < 0$, the plasma electrons are flowing backward, $u_f = -\phi_0 \cos\psi < 0$, and the electric field is accelerating, $E_z/E_0 = \phi_0 \sin\psi < 0$. Here $\epsilon < 0$ and the beat wave buckets open to the right (see Fig. 2). Consider an electron that is initially flowing backward and resides below the beat wave separatrix. Since the separatrix opens to the right, there exists open orbits which can take an electron from below to above the beat wave separatrix. Such an electron can acquire a sufficiently large positive velocity to allow trapping and acceleration in the plasma wave. These open phase space orbits, which provide the necessary path for electron acceleration, can exist when the beat wave resides within $-\pi/2 < \psi < 0$.

An estimate for the threshold for injection into the wakefield can be obtained by considering the effects of the wakefield and the beat wave individually and by requiring (i) the maximum energy of the beat wave separatrix exceed the minimum energy of the wakefield separatrix, $u_{bmax} \geq (\Delta\phi^{-1} - \Delta\phi)/2$, and (ii) the minimum momentum of the beat wave separatrix be less than the plasma electron fluid momentum, $u_{bmin} \leq -\phi$, where u_{bmax}, u_{bmin} are given by Eq. (5) with $\epsilon = 0$. These two conditions (illustrated schematically in Fig. 2) imply that the beat wave separatrix overlaps both the wakefield separatrix and the plasma fluid oscillation, thus providing a phase-space path for plasma electrons to become trapped in the wakefield. For a given wakefield amplitude ϕ_0, conditions (i) and (ii) imply the optimal phase location $3\phi_0 \cos\psi \simeq 3^{1/2} - 2\phi_0 - 2\beta_{pb}$ and threshold amplitude $6\hat{a}_1 > 3^{1/2} - 2\phi_0 + \beta_{pb}$ of the injection pulse, where $\phi_0^2 \cos^2\psi \ll 1$, $\hat{a}_1^2 \ll 1$, and $\beta_{pb}^2 \ll 1$

were assumed. For example, $\phi_0 = 0.6$ and $\beta_{pb} = 0.05$ imply $\psi = -1.3 - 2\pi j$ and $\hat{a}_1 > 0.11$.

To further evaluate the colliding laser injection method, the motion of test particles in the combined wake and laser fields was simulated by numerically solving Eq. (2). At $\tau = 0$, the forward (backward) pulse profile $\hat{a}_1$ ($\hat{a}_2$) is a half-period of a sine wave with maximum amplitude a_{1m} (a_{2m}), centered at $\psi = \psi_1 < 0$ ($\psi_2 > 0$), with length L_1 (L_2). Test particles are loaded uniformly from $\psi = 0$ to $\psi = \psi_{max}$ with $d\psi/d\tau = -\beta_{p0}$ (initially at rest) and pushed from $\tau = 0$ to $\tau = \tau_{max}$. In the simulations, $\omega_1/\omega_p = 100$, $\omega_2/\omega_p = 90$, and $\phi_0 = 0.6$, which for $\lambda = 2\pi c/\omega_1 = 1$ μm implies $n_0 \simeq 10^{17}$ cm^{-3} and $E_z = 0.6E_0 \simeq 19$ GV/m. Also, $\hat{\phi} = \phi_0 \left[1 - \exp(-\psi^2/\pi^2)\right]$ for $\psi \leq 0$.

Figure 3(a) shows a phase space plot (u_z versus ψ) of the trapped electrons at $\tau_{max} = 300$ (0.48 cm) for $a_{1m} = a_{2m} = 0.3$ (1.2×10^{17} W/cm^2), $L_1 = L_2 = \lambda_p/8$ (42 fs), $\psi_1 = -13.6$ and $\psi_2 = 21.4$ (chosen so the beat wave and test particles overlap). The trapped electrons have an average momentum $\langle u_z \rangle = 116$ (59 MeV), with a standard deviation spread $\delta u_z/\langle u_z \rangle = 0.21$; however, 60% of the electrons are contained within 66 MeV $\pm 8\%$, as evident from Fig. 3(b). The electrons are centered at $\psi = -14.97$ with a standard deviation $\delta\psi = 0.199$, which gives a bunch length $L_b = 6.3$ μm (21 fs). Note that the electrons have a time-correlated energy spread (chirp), as can be the case in Ref. [8]; hence, compression techniques can be used to further shorten the bunch length.

Simulations indicate that trapping occurs when the center of the $L_1 = \lambda_p/8$ pulse is located from $-14.2 \leq \psi_1 \leq -13.5$. This implies that the forward pulse must be synchronized to the wakefield with an accuracy < 37 fs, which is not a serious constraint and can be relaxed somewhat by using a longer forward pulse. Furthermore, simulations show that

$\langle u_z \rangle$ and $\delta u_z / \langle u_z \rangle$ are relatively insensitive to variations in $L_{1,2}$, e.g., $L_1 = L_2 = \lambda_p/2$ give results similar to those of Fig. 3. This is the case when a_{1m} is well above threshold (as in Fig. 3). The observed momentum spread can be traced to the half-sine pulse profiles, which implies that different electrons encounter different beat wave amplitudes and are injected into the wakefield with different energies.

Figure 4 summarizes simulations in which the injection pulse amplitudes $a_{1m} = a_{2m}$ were varied. Parameters are the same as in Fig. 3 except that $\psi_1 = -13.8$ and $\psi_2 = 21.5$. This ψ_1 value was carefully optimized and agrees well with the analytical prediction. Plotted as functions of a_{1m} are the maximum u_{zm}, average $\langle u_z \rangle$, and spread $\delta u_z / \langle u_z \rangle$ in the momenta, and the fraction f_{tr} of those particles which encounter the beat wave that become trapped. Trapping is observed for $a_{1m} > 0.17$, but the beam energy and trapping fraction improve substantially as a_{1m} is raised above 0.25. The simulation threshold for a_{1m} is somewhat higher than the analytical prediction (0.11).

The bunch density is $n_b \simeq f_{tr} n_0 L_z / L_b$, where $L_z \simeq (L_1 + L_2)/2$ is the length of plasma that encounters the overlapping pulses. Assuming that the 1-D results hold for a pump laser of radius r_0 implies a total number of trapped electrons $N_b \simeq f_{tr} n_0 L_z \pi r_0^2$, e.g., $n_b \simeq 10^{17}$ cm^{-3} and $N_b \simeq 10^9$ for Fig. 3 with $r_0 = 40$ μm. Note that N_b can be increased by increasing n_0, r_0, a_{1m} (via f_{tr}) and, in particular, L_z by increasing the duration of the backward pulse L_2. The ratio of N_b to the theoretical beam loading limit N_0 [12] is $N_b/N_0 = f_{tr} k_p L_z E_0 / E_z$, which can easily approach unity. For N_b near N_0, however, space-charge effects become important and a self-consistent simulation is required.

In summary, a method has been proposed and analyzed for injecting plasma electrons into a large (> 10 GeV/m) wakefield using two colliding laser pulses: a forward injection pulse and a backward injection pulse of lower frequency. When the injection pulses collide, a slow ($v_{pb} \ll c$) ponderomotive wave is generated that injects plasma electrons into the fast ($v_{p0} \simeq c$) wakefield for acceleration to high energy. The optimal phase location and threshold amplitude of the injection pulse were determined, e.g., injection pulse intensities of 5×10^{16} W/cm^2 for a wakefield amplitude of $\delta n/n = 0.6$. Simulations of test electrons in prescribed 1-D fields indicate that short (≤ 20 fs), high density ($\geq 10^{17}$ cm^{-3}), relativistic (≥ 50 MeV) electron bunches can be obtained with energy spreads $\leq 20\%$.

The authors acknowledge useful conversations with T. Antonsen, J.L. Bobin, T. Katsouleas, P.B. Lee, W.B. Mori, C. Schroeder, G. Shvets, and D. Umstadter. This work was supported by the Department of Energy and the Office of Naval Research.

References

[1] For a recent review, see E. Esarey et al., IEEE Trans. Plasma Sci **PS-24**, 252 (1996).

[2] J.R. Marques et al., Phys. Rev. Lett. **76**, 3566 (1996); C.W. Siders et al., Phys. Rev. Lett. **76**, 3570 (1996); A. Ting et al., Phys. Rev. Lett. **77**, 5377 (1996); S.P. LeBlanc et al., Phys. Rev. Lett. **77**, 5381 (1996).

[3] K. Nakajima et al., Phys. Rev. Lett. **74**, 4428 (1995); C. Coverdale et al., Phys. Rev. Lett. **74**, 4659 (1995); D. Umstadter et al., Science **273**, 472 (1996); A. Modena et al., Nature **377**, 606 (1995).

[4] A. Ting et al., Phys. Plasmas, accepted (1997).

[5] T. Tajima and J.M. Dawson, Phys. Rev. Lett. **43**, 267 (1979); P. Sprangle et al., Appl. Phy. Lett. **53**, 2146 (1988); L.M. Gorbunov and V.I. Kirsanov, Sov. Phys. JETP **66**, 209 (1987).

[6] P. Sprangle et al., Phys. Rev. Lett. **69**, 2200 (1992); T.M. Antonsen and P. Mora, Phys. Rev. Lett. **69**, 2204 (1992); N.E. Andreev et al., JETP Lett. **55**, 571 (1992); E. Esarey et al., Phys. Fluids B **5**, 2690 (1993).

[7] W.B. Mori et al., Phys. Rev. Lett. **72**, 1482 (1994); E. Esarey, J. Krall, and P. Sprangle, Phys. Rev. Lett. **72**, 2887 (1994); N.E. Andreev, V.I. Kirsanov, and L.M. Gorbunov, Phys. Plasmas **2**, 2573 (1995).

[8] D. Umstadter, J.K. Kim, and E. Dodd, Phys. Rev. Lett. **76**, 2073 (1996).

[9] C. Joshi et al., Phys. Rev. Lett. **47**, 1285 (1981); D.W. Forslund et al., Phys. Rev. Lett. **54**, 558 (1985).

[10] P. Bertrand et al., Phys. Rev. E **49**, 5656 (1994); Phys. Plasmas **2**, 3115 (1995).

[11] E. Esarey and M. Pilloff, Phys. Plasmas **2**, 1432 (1995).

[12] T. Katsouleas et al., Particle Accelerators **22**, 81 (1987).

Figure Captions

Fig. 1: Profiles of the pump laser pulse a_0, the wakefield ϕ, and the forward a_1 injection pulse, all of which are stationary in the $\psi = k_p(z - v_{p0}t)$ frame, and the backward injection pulse a_2, which moves to the left at $\simeq 2c$.

Fig. 2: Schematic of phase space, u_z versus ψ, showing the wakefield separatrix u_{min}, the electron motion in the wakefield u_f, and a single beat wave separatrix u_b (the width greatly exaggerated).

Fig. 3: Trapped electrons from a simulation with $\omega_1/\omega_p = 100$, $\omega_2/\omega_p = 90$, $\phi_0 = 0.6$, $a_{1m} = a_{2m} = 0.3$, and $L_1 = L_2 = \lambda_p/8$: (a) phase space, $u_z = p_z/m_e c$ versus ψ, with the injection pulse (solid curve) and wakefield (dashed curve) profiles; and (b) electron distribution $f(E)$ per 2 MeV energy bin.

Fig. 4: The maximum u_{zm}, average $\langle u_z \rangle$, and spread $\delta u_z/\langle u_z \rangle$ in the momenta, and the fraction f_{tr} of trapped electrons as functions of $a_{1m} = a_{2m}$, for the parameters of Fig. 3 with $\psi_1 = -13.8$.

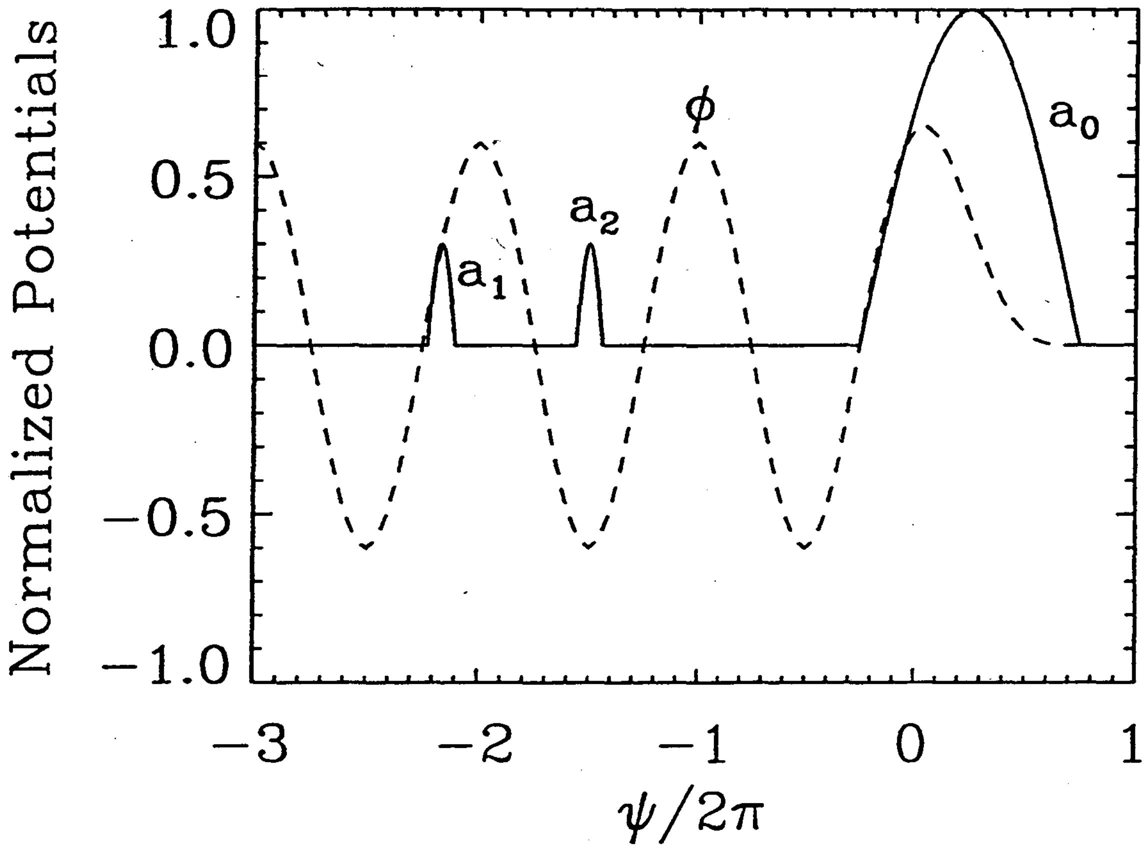

Normalized Potentials
1.0
0.5
0.0
−0.5
−1.0
−3
−2
−1
0
1
$\psi/2\pi$
ϕ
a_0
a_1
a_2

Fig. 1

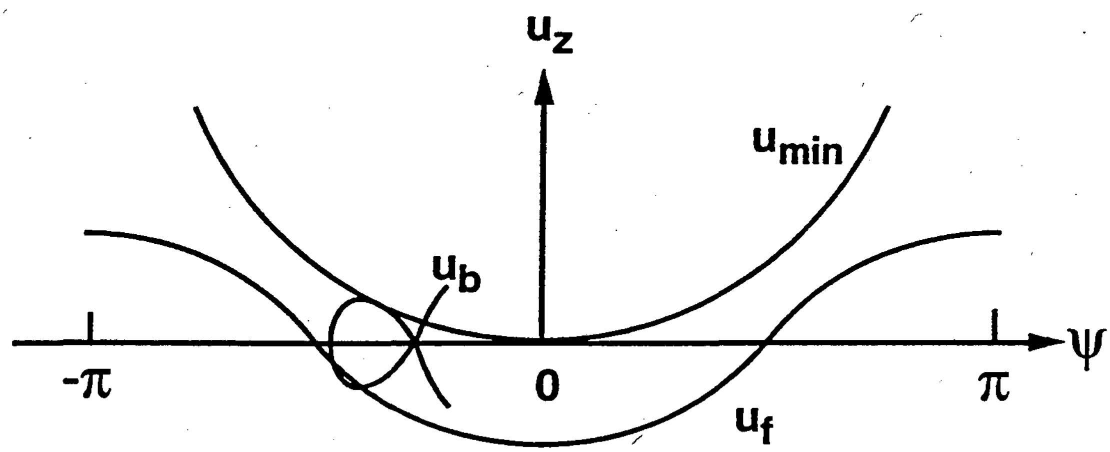

Fig. 2

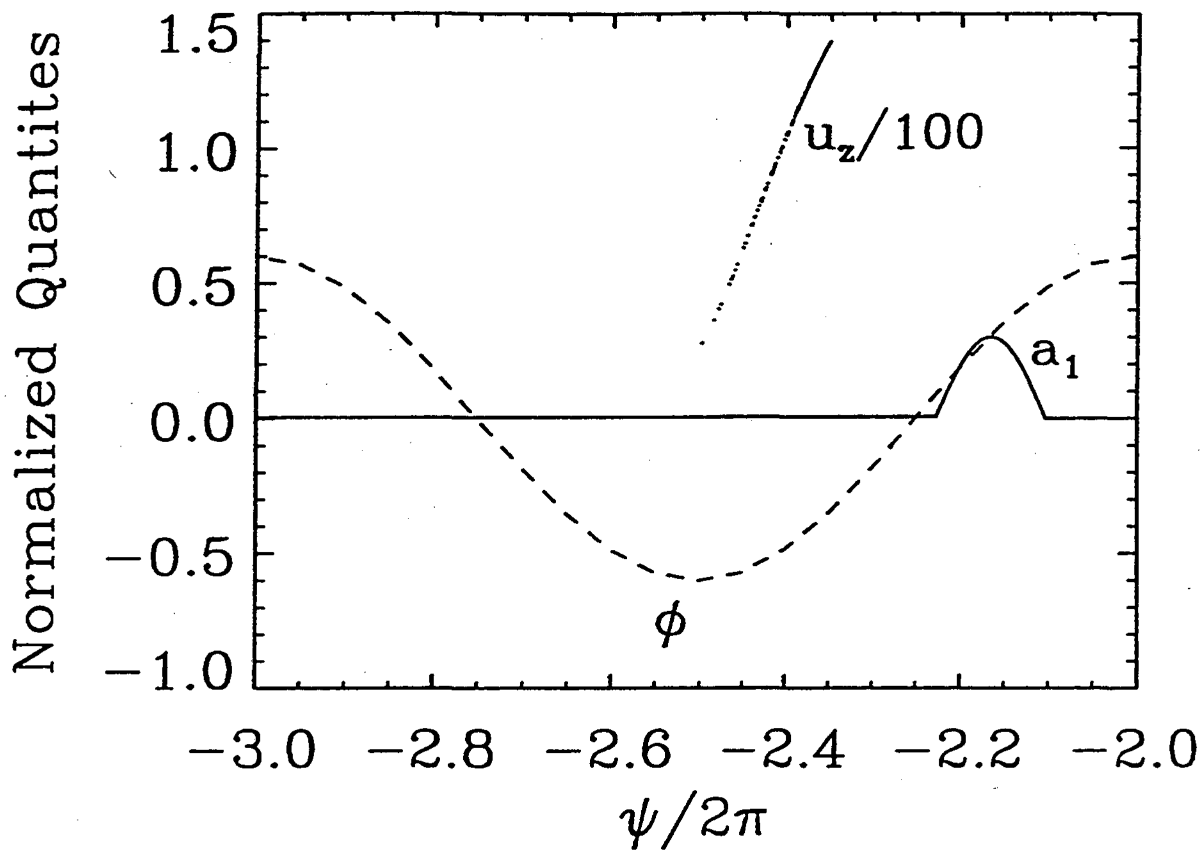
Normalized Quantites
1.5
1.0
0.5
0.0
−0.5
−1.0
$u_z/100$
a_1
ϕ
−3.0
−2.8
−2.6
−2.4
−2.2
−2.0
$\psi/2\pi$

Fig. 3(a)

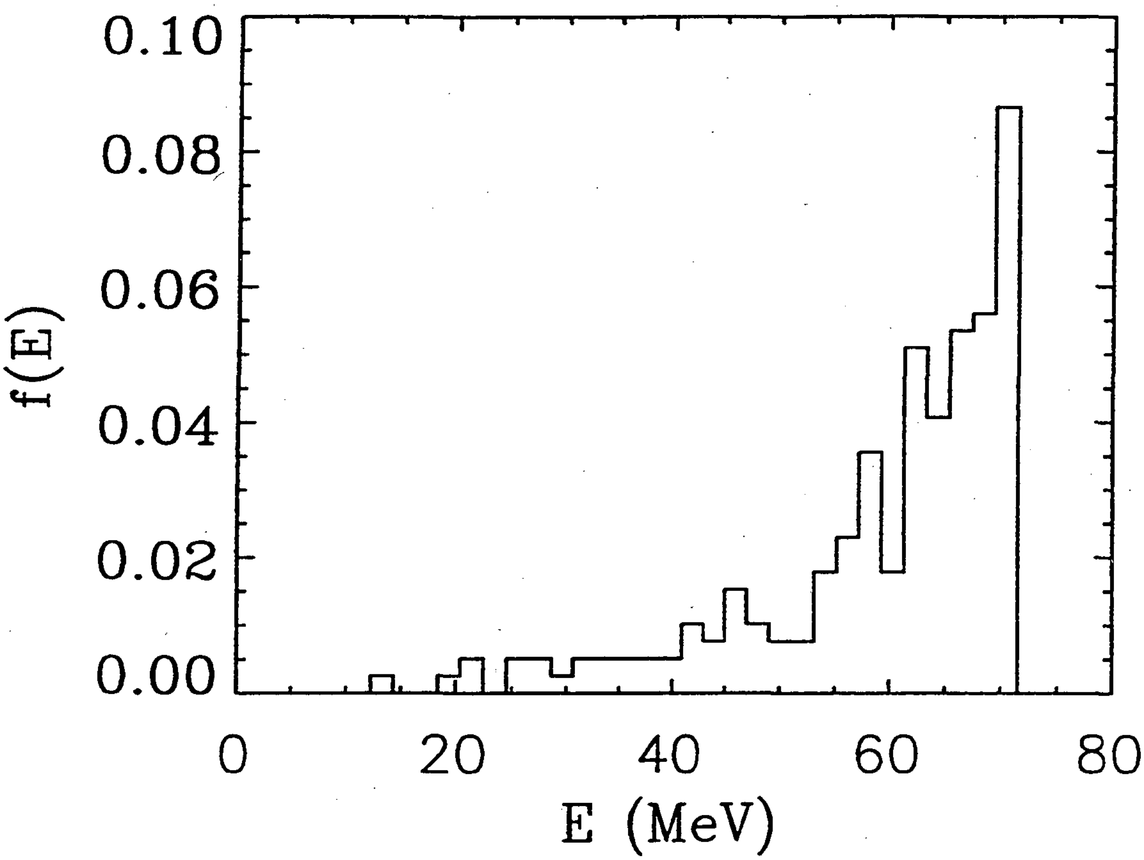

Fig. 3(b)

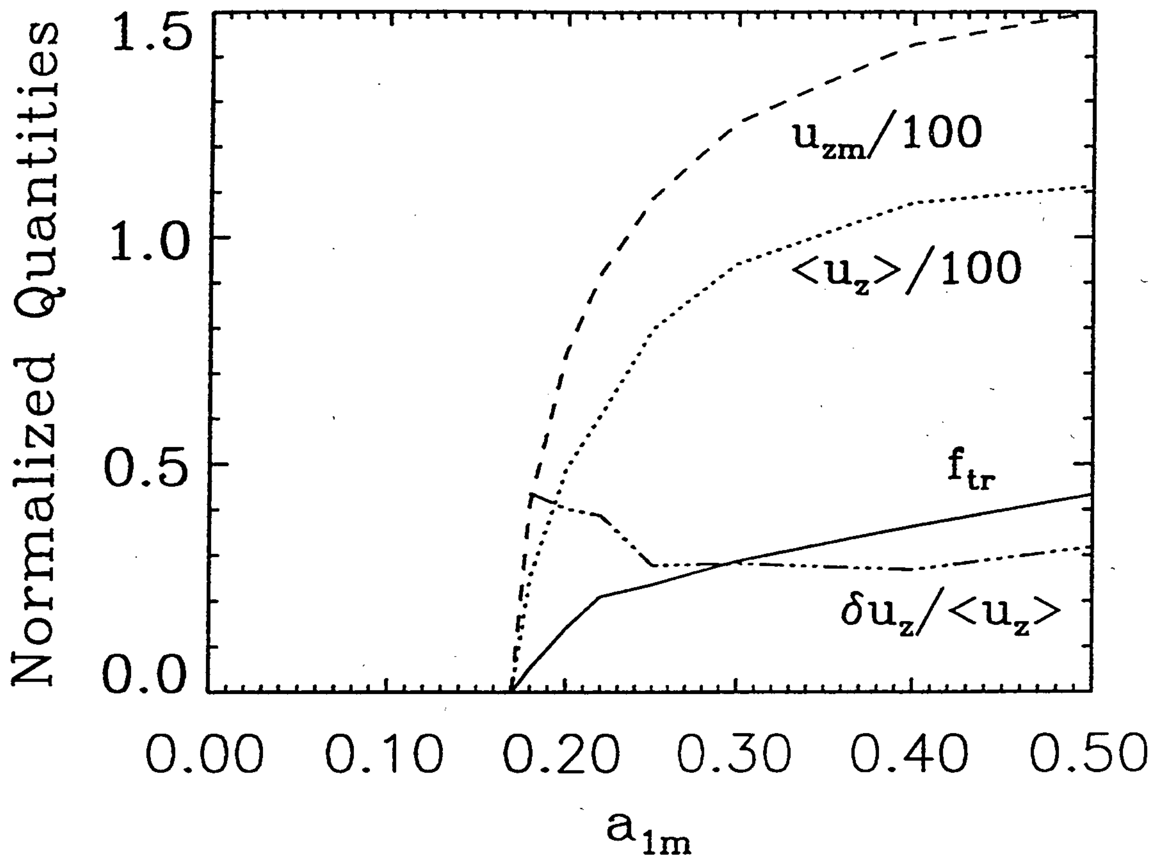

Normalized Quantities
1.5
1.0
0.5
0.0
0.00
0.10
0.20
0.30
0.40
0.50
a_{1m}
$u_{zm}/100$
$<u_z>/100$
f_{tr}
$\delta u_z/<u_z>$

Fig. 4

ERNEST ORLANDO LAWRENCE BERKELEY NATIONAL LABORATORY
ONE CYCLOTRON ROAD | BERKELEY, CALIFORNIA 94720

Prepared for the U.S. Department of Energy under Contract No. DE-AC03-76SF00098